Plasmid-encoded H-NS controls extracellular matrix composition in a modern *Acinetobacter baumannii* urinary isolate

Saida Benomar[a#], Gisela Di Venanzio[a], Mario F. Feldman [a#]

[a] Department of Molecular Microbiology, Washington University School of Medicine, St Louis, MO, 63110, USA.

[#] Address correspondence to Saida Benomar, sbenomar@wustl.edu, or Mario F. Feldman, mariofeldman@wustl.edu

Running title: Biofilm regulation in *Acinetobacter baumannii* by H-NS

ABSTRACT

Acinetobacter baumannii is emerging as a multidrug-resistant (MDR) nosocomial pathogen of increasing threat to human health worldwide. The recent MDR urinary isolate UPAB1 carries the plasmid pAB5, a member of a family of large conjugative plasmids (LCP). LCP encode several antibiotic resistance genes and repress the type VI secretion system (T6SS) to enable their dissemination, employing two TetR transcriptional regulators. Furthermore, pAB5 controls the expression of additional chromosomally encoded genes, impacting UPAB1 virulence. Here we show that a pAB5-encoded H-NS transcriptional regulator represses the synthesis of the exopolysaccharide PNAG and the expression of a previously uncharacterized three-gene cluster that encodes a protein belonging to the CsgG/HfaB family. Members of this protein family are involved in amyloid or polysaccharide formation in other species. Deletion of the CsgG homolog abrogated PNAG production and Cup pili formation, resulting in a subsequent reduction in biofilm formation. Although this gene cluster is widely distributed in Gram-negative bacteria, it remains largely uninvestigated. Our results illustrate the complex cross-talks that take place between plasmids and the chromosomes of their bacterial host, which in this case can contribute to the pathogenesis of *Acinetobacter.*

IMPORTANCE

The opportunistic human pathogen *Acinetobacter baumannii* displays the highest reported rates of multidrug resistance among Gram-negative pathogens. Many *A. baumannii* strains carry large conjugative plasmids like pAB5. In recent years, we have witnessed an increase in knowledge about the regulatory cross-talks between plasmids and bacterial

chromosomes. Here we show that pAB5 controls the composition of the bacterial extracellular matrix, resulting in a drastic reduction in biofilm formation. The association between biofilm formation, virulence, and antibiotic resistance is well-documented. Therefore, understanding the factors involved in the regulation of biofilm formation in *Acinetobacter* has remarkable therapeutic potential.

INTRODUCTION

Acinetobacter baumannii is regarded as a nosocomial pathogen capable of causing multiple types of infection; however, in the last few years community-acquired infections have become more common. Importantly, *A. baumannii* is a major threat to global health due to the increasing prevalence of the multi-drug resistant (MDR) isolates (1,2). Genes encoding for antibiotic resistance are usually located in chromosomal resistance islands or in plasmids (3,4). Plasmids are major contributors to horizontal gene transfer (HGT), as they facilitate the exchange of genetic material between microorganisms, spreading the MDR phenotype (5-7). For decades, plasmid biology focused on their replication, maintenance, and mobilization, as well as their contribution to antibiotic resistance and virulence (8). More recently, genomic and transcriptomic analyses have begun to uncover complex and dynamic relationships between plasmids and their host chromosome.

A. baumannii strains harbor different types of plasmids. Regarding MDR, the Large Conjugative Plasmids (LCPs) family, which are approximately 150-200 Kb, are particularly worrisome. pAB3, the LCP carried in the lab strain ATCC17978, isolated in 1951 carries only one cassette conferring resistance to trimethoprim. However, pAB04 or pAB5, LCPs from recent clinical isolates AB04 and UPAB1, contain 12 and 15 antibiotic resistance cassettes, respectively. This increase in the number of antibiotic resistance cassettes illustrates the rapid evolution of these plasmids. LCPs contain three conserved regions: the MDR region, containing various antibiotic resistance cassettes; a region encoding the T4SS conjugative pilus, required for plasmid dissemination via conjugation; and the regulatory region, which contains several transcriptional regulators (9-11). For example, LCPs harbor two TetR regulators that repress the Type VI secretion system (T6SS) encoded in *A.*

baumannii chromosome, which allows conjugation and promotes their own dissemination (10).

We have previously shown that besides providing resistance to antibiotics and repressing T6SS, pAB5 can control the expression of additional chromosomally encoded genes, impacting UPAB1 virulence (11). The regulatory activity of pAB5 can be observed by plating cells with or without this plasmid in Congo-red containing plates. The bacteria colonies carrying pAB5 are much lighter, which reflects a clear reduction in Congo-red binding. Transcriptomic and proteomic analysis revealed that pAB5 reduced the expression of cell-surface components, including (Chaperone/Usher Pathway) CUP pili, β-1 → 6-linked poly-N-acetyl glucosamine (PNAG), and many additional proteins of unknown functions (11). A bioinformatic analysis of the pAB5 sequence revealed that this LCP encodes at least six genes predicted to function as transcriptional regulators. In this work, we explored the cross-talk between pAB5 and the chromosome of UPAB1, and identified the transcriptional regulator involved in regulation of PNAG synthesis. Furthermore, our analysis revealed a novel uncharacterized gene cluster regulated by pAB5, evolutionarily related to curli formation, and whose disruption has a dramatic effect on the surface composition of UPAB1.

RESULTS

The transcriptional regulator H-NS, from pAB5, controls UPAB1 phenotype on Congo red binding. We have recently shown that pAB5 regulates the expression of multiple chromosomally encoded virulence factors in UPAB1 (11). One of the most evident phenotypes controlled by pAB5 is congo-red binding, which has been associated to the

111 presence of either amyloid fibers, such as curli, or polysaccharides in *Escherichia coli* and
112 *A. baumannii* species (ref). pAB5 encodes at least six putative transcriptional regulators
113 (table S1). Among these, there are two TetR regulators, TetR1 and TetR2, virtually identical
114 to the ones encoded in plasmid pAB3. These two TetR regulators inhibit the assembly of
115 the type VI secretion system (T6SS) machinery, which is employed by multiple
116 *Acinetobacter* strains to compete with other bacteria (9,10). pAB5 carries one additional
117 regulator of unknown function, belonging to the TetR family, TetR3. In addition, pAB5
118 encodes the global regulator H-NS (histone-like nucleoid structuring). H-NS-like proteins
119 have been shown to be implicated in the facilitation of chromosome evolution through their
120 ability to silence transcription, allowing integration of horizontally transferred genes into
121 bacterial chromosomes (12). Finally, orthologues of other regulators, such a FrmR, a
122 putative metal/formaldehyde-sensitive transcriptional repressor, and ArsR, a putative
123 repressor belonging to the arsenic-sensitive family transcriptional regulators are also
124 encoded in pAB5. To investigate if any of these regulators' controls Congo red binding, we
125 cloned them individually in the pVRL2 expression vector (13). The constructs were
126 transformed into UPAB1p-, and the different strains were platted on Congo red plates. As
127 previously reported, UPAB1 displayed a reduced Congo-red binding (white colonies)
128 compared to UPAB1p- (red colonies), which correlated with the quantification of Congo red
129 binding (fig 1A and B). From the six regulators expressed in UPAB1p-, only H-NS changed
130 the color of the colonies and diminished congo-red binding (fig 1A and B). All other strains
131 expressing the remaining five regulators behaved as UPAB1p-, exhibiting similar leveles of
132 Congo red binding. Finally, UPAB1Δ*h-ns*, a strain carrying pAB5 without *h-ns*, showed
133 comparable levels of Congo-red binding to UPAB1p- (fig 1C and D). These results

demonstrate that H-NS is solely responsible for the pAB5-dependent repression of Congo-red binding.

Plasmid-encoded H-NS inhibits PNAG production. It has been proposed that in some *A. baumannii* strains, Congo-red binding is linked to PNAG production (14). To examine if pAB5 inhibits PNAG production, we used a specific antibody to check for the presence or absence of PNAG. In correlation to congo red phenotypes, UPAB1 and UPAB1p- expressing *h-ns* (p-/*h-ns*) showed drastically reduced levels of PNAG production while UPAB1p-, UPAB1p- harboring the empty vector (p-/vec) and UPAB1Δ*h-ns* strains show similar level of PNAG production (fig 2A). The differences observed on the levels of PNAG production were not related to differences on cells loaded to the membrane (fig 2B). None of the other putative transcriptional regulators from pAB5, altered PNAG-production (fig S1). The locus containing the *pgaABCD* genes has been shown to be responsible for PNAG production in the clinical isolate *A. baumannii* S1 (14). UPAB1 harbors a similar gene cluster containing four genes *pgaABCD* (fig 3A). The pgaA-D cluster encodes for the poly-beta-1,6 N-acetyl-D-glucosamine export porin PgaA; the poly-beta-1,6-N-acetyl-D-glucosamine N-deacetylase PgaB, the poly-beta-1,6 N-acetyl-D-glucosamine synthase PgaC, and the poly-beta-1,6-N-acetyl-D-glucosamine biosynthesis protein PgaD (15). These proteins have an identity ranging from 23 to 55 % to the PNAG cluster in *E. coli* and *Yersinia pestis*. Our recent transcriptomic data showed that this locus is repressed by pAB5 (11). By RT-PCR, we show that expression of *pgaABC* was repressed by H-NS (fig 3B). Furthermore, the pgaA mutant or the whole *pgaA-D* mutant abolished Congo red binding (fig 4A and S2) and PNAG production (fig 4 B,C). These phenotypes were recovered in the complemented strains, demonstrating that *pgaA-D* is responsible for PNAG production in UPAB1. Together, these

157 results show that H-NS downregulates the *pgaA-D* cluster with the concomitant repression
158 in PNAG production.

159 **H-NS regulates the expression of a previously unidentified "curli-like" cluster.** Congo-
160 red binding has been routinely employed to monitor Curli amyloid production in *E. coli*. In
161 this bacterium, curli synthesis involves two operons, *csgBAC* and *csgDEFG*. These operons
162 are responsible for curli fiber polymerization, stability, transport and assembly (16-18).
163 Particularly, CsgG forms an oligomeric transport complex and is essential for curli assembly.
164 Although curli formation has not been reported in *Acinetobacter* species, a bioinformatic
165 analysis revealed that a CsgG ortholog (D1G37_12595) is contained within a gene cluster
166 that also comprises two additional genes, D1G37_12600 ("Ab12600") and D1G37_12605
167 ("Ab12605"), both encoding putative lipoproteins (fig 5A). Our previous transcriptomic and
168 proteomic analysis indicated that these genes are also downregulated by pAB5 (11). We
169 validated these data by RT-PCR and determined that the transcription of *csgG* and Ab12600
170 is repressed ~10 fold by pAB5 or a vector expressing *h-ns* (fig 5B), indicating that, besides
171 PNAG, H-NS also represses the csgG curli-like cluster in UPAB1.

172 **Disruption of CsgG decreases PNAG production, Cup pili formation and biofilm**. To
173 explore the role of the CsgG-containing operon in UPAB1, we deleted the *csgG* and 12600
174 genes in the strains expressing high levels of *csgG*, i.e., UPAB1p- and UPAB1Δ*h-ns*.
175 Surprisingly, *csgG* and 12600 mutant strains showed low levels of Congo-red binding and
176 reduced PNAG production, similar to the *pgaA-D* and *pgaA* mutants, (fig 4A, B and S2). The
177 complementation of the two mutants rescued both phenotypes. To further explore the role
178 of the Curli-like cluster, we analyzed these cells via SEM and TEM. SEM images showed
179 that UPAB1p- cells were coated with a thick layer of extracellular matrix material (fig 6). The

csgG mutant displayed drastically reduced attachment to the coverslip and, except for some fibers, lacked most of the extracellular matrix (fig 6). This phenotype was partially complemented by expressing the CsgG gene *in trans*. (fig 6). For comparative purposes, we also examined the Δ*pgaA-D* mutant strain. The Δ*CsgG* and Δ*pgaA-D* strains exhibited similar phenotypes, although the reduced binding to the coverslips was less pronounced in the Δ*pgaA-D* strain (fig 6). These phenotypes are not due to growth defects (fig S4), and they correlate with the lower PNAG production in the *csgG* mutant. Our TEM analysis showed that CsgG, but not PgaA-D deletion, results in an almost total abrogation of CUP pili formation (fig 7). CUP pili levels were restored in the complemented cells. Western-blot analysis confirmed that deletion of CsgG abrogated CUP pili expression (Fig S4). Moreover, this analysis confirmed that CUP pili is repressed by pAB5, although this repression was independent of H-NS (Fig S4). The changes in the extracellular matrix were also reflected in the levels of biofilm formation, as the *pgaA-D* and *csgG* mutants produced less biofilm compared to wild-type bacteria (Fig 8). The reduction of biofilm formation was restored in the complemented strains (fig S5). Moreover, cells carrying pAB5, but not pAB5Δ*h-ns*, displayed lower levels of biofilm formation. Together these experiments demonstrate that deletion of CsgG results in reduced production of PNAG and CUP pili, with the subsequent reduction in biofilm formation.

The *csgG* cluster is widely distributed in Gram-negative bacteria. Our results show that CsgG is implicated in different phenotypes in UPAB1. A bioinformatics analysis revealed that this cluster is widespread among Gram-negative bacteria (fig 9). In some bacterial species, such as *Neisseria meningitidis* or *Vibrio harveyi*, the locus contains additional genes predicted to be co-transcribed. Recently, the crystal structure of GNA1162 from *N.*

meningitidis, a homologue to D1G37_12605, has been solved (21). GNA 1162 exhibited structural similarities to TolB, and authors speculate that this protein may act as an accessory protein to an unidentified transport machinery. Despite, this cluster is present in a very large number of bacteria, its roles remain unknown and further studies are needed to identify the target of this cluster and its importance in virulence.

DISCUSSION

We have previously shown that the *Acinetobacter* LCPs play a key role in the dissemination of MDR and influences the pathogenesis of this bacterium by controlling the expression of chromosomally-encoded virulence factors. In this study, we show that pAB5, the LCP from UPAB1, encodes a H-NS transcriptional regulator that inhibits biofilm formation by repressing the expression of PNAG. Additionally, we found that pAB5-encoded HN-S represses the expression of a three-gene cluster that contains a homolog of CsgG, a protein involved in curli assembly. We found that disruption of CsgG dramatically reduced PNAG production, CUP pili assembly, and consequently, biofilm formation. Bioinformatic analysis revealed that the “curli like cluster” is widely distributed among Gram-negative bacteria without any attributed function.

The cross-regulatory pathways between plasmids and the bacterial chromosomes have been recently reviewed (22). Plasmid-encoded transcriptional regulators can modulate the expression of genes involved in many different processes, including motility, glycogen synthesis, adherence and quorum sensing, among others (22). H-NS-like proteins are encoded in plasmids in *Shigella flexneri* and *Salmonella enterica*. However, in these species, plasmid-encoded H-NS appear to regulate only genes horizontally acquired which

maintain the energetic cost of their expression at a lower level, without affecting expression of other chromosomal genes (22). We have previously shown that repressing chromosomally encoded T6SS enable the dissemination of LCPs via conjugation (10). By downregulating PNAG, CsgG, and CUP pili, pAB5 represses biofilm formation in UPAB1. In monospecies biofilms, bacteria are surrounded by their kin, which limits the dissemination capacity of the plasmids. It is tempting to speculate that promoting the planktonic lifestyle of the host increases the chances of dissemination of pAB5 to other bacterial hosts. However, further work is required to understand the physiological implication of this process.

Our discovery that pAB5-encoded H-NS represses biofilm formation in UPAB1 is preceded by similar findings in *E. coli* and *Salmonella* (23-28). However, in these species H-NS is encoded in the chromosome. In *E. coli* and *Salmonella*, the CsgG protein is part of a multi protein complex responsible for curli fiber formation, and H-NS regulates its expression by repressing *csgD*, a key regulator for curli synthesis. In these species, H-NS is part of an intricate regulatory network that integrates diverse environmental conditions and ultimately controls curli biogenesis. CsgG is part of a predicted operon together with two putative lipoproteins of unknown function that is widely distributed in Gram-negative bacteria. *Acinetobacter* spp does not encode a complete curli biosynthetic machinery and curli fibers have not been reported. In *Caulobacter,* the CsgG ortholog, named HfaB is part of a cluster containing HfaABD, where HfaA has properties of amyloid proteins (CsgA). The HfaABD complex is critical for anchoring holdfast, a polysaccharide made of N-acetyl-d-glucosamine (NAG), and other sugars to the *Caulobacter* cell surface. It has been proposed that holdfast is attached to HfaA by an unknown mechanism (29-31). We hypothesize that a similar function anchoring PNAG to the cell surface is accomplished by a multimeric complex

249 formed by CsgG and the two lipoproteins in the operon. Further work is necessary to
250 determine the exact role of this gene cluster in the assembly of the extracellular matrix in
251 these species.

252

253 **MATERIALS AND METHODS**

254 **Bacterial strains and growth conditions.** Bacterial strains, plasmids, and oligonucleotides
255 used in this study are listed in Supplementary information. Unless otherwise noted, all
256 strains were grown in Lysogeny broth (LB) broth at 37C with shaking (200 rpm). For strain
257 constructions, we used gentamicin (15 or 20 μg ml^{-1}), kanamycin (7.5 or 50 μg ml^{-1}), zeocin
258 (50 μg ml^{-1} with low salt LB), hygromycin (300 μg ml^{-1}).
259 **Construction of *A. baumannii* mutants and complement strains, and pVRL2**
260 **constructs**. Plasmids, and oligonucleotides used in this study are listed in Supplementary
261 Tables S2 and S3, respectively. The constructs for generating deletions in *h-ns*, *pgaA-D*,
262 *pgaA*, *csgG* and D1G37_126000 were made by substitution of the gene by an antibiotic
263 (kanamycin or zeocin) cassette as described previously (32). Selection of mutants was
264 carried out using the proper antibiotic. To make unmarked strains, electrocompetent
265 mutants were transformed with pAT03 to remove the FRT-flanked antibiotic cassette.
266 Transformants were plated on LB-agar plates containing 2 mM IPTG + hygromycin to
267 express FLP recombinase. All strains were verified by antibiotic resistance, PCR
268 amplification and gene sequencing. To generate genetic complementation, genes of interest
269 were cloned into the pUC18T-miniTn7T-Gm (zeo) vector and introduced to UPAB1p- strains
270 via four-parental mating methods as described previously (33,34). Briefly, 100 μl of

stationary cultures was normalized to an OD600 of 2.0 of each recipient strain, and HB101(pRK2013), EC100D(pTNS2), and EC100D containing the pUC18T-miniTn7T constructs were added to 600 μl of warm LB. Each suspension was washed twice by centrifugation at 7000g, followed by resuspension of the bacterial pellet in 1 ml of warm LB. On the final wash, the bacterial pellet was resuspended in 25 μl of LB, and the suspension was spotted on a prewarmed LB agar plate (or low-salt LB agar plate) and incubated overnight at 37°C. The bacteria were scraped from the plate, resuspended in 1 ml of LB, vortexed, and serial dilutions were plated on L agar plates supplemented with chloramphenicol to select against *E. coli* strains and gentamicin or zeocin to select for *A. baumannii* strains that had received the mini-Tn7 constructs. Correct insertion of the constructs was verified by PCR amplification and sequencing. The expression of different regulators of the pAB5 plasmid as p/*h-ns*, p/*tetR*1 and others were made using the pVRL2 vector (13). Constructs were generated by restriction enzime cloning using the HindIII and PstI sites. All the constructs were introduced to UPAB1p- strains by electroporation and transformants were selected on gentamicin.

Congo red plate and congo red binding quantification. The red versus white color of cells was investigated using YESCA agar media (35) supplemented with 50 μg/ml Congo red. To quantify the congo red binding for bacteria prestained on the YESCA congo red plates (36). Cells were recovered from YESCA congo red plates after incubation at 26C for 48 hours. Cells were washed twice in 50 mM potassium phosphate buffer by centrifugation at 16,000 x g for 2 min and resuspended in 1 ml 50 mM potassium phosphate buffer, and the OD was adjusted to 1.100 μl of each sample were loaded onto a 96-well opaque plate, the fluorescence of congo red was measured using the plate reader (BioTek microplate

spectrophotometer) with an excitation wavelength at 485nm and emission at 612 nm. The buffer was used as the blank.

Reverse transcription-PCR. Cells were taken from LB plates after an overnight growth at 26°C and normalized to OD 1 and treated with RNA protect. RNA purification was prepared using the Quick RNA fungal/bacterial miniprep (Zymo Research) by following the manufacturer's instructions with some modification in the DNA digestion step as follows. Contaminating DNA was removed using the Turbo DNA-free kit (Invitrogen) by following the manufacturer's instructions. For reverse transcription (RT)-PCR, cDNA was prepared from 1 μg RNA using a high-capacity RNA-to-cDNA kit (Applied Biosystems), according to the manufacturer's protocol. Real-time quantitative PCR (qPCR) was performed using Power SYBR green PCR master mix reagents (Applied Biosystems) on a ViiA7 real-time PCR system (Applied Biosystems), following the manufacturer's suggested protocol. In all cases a no-template control was run with no detectable transcripts.

Biofilm formation. Cells were grown overnight in 5 ml of LB broth (or YESCA), then cultures were diluted to an OD600 of 0.01 in LB broth (or YESCA). Cultures were deposited in 96-well plates and incubated at 37 °C for 8 or 24 hours without shaking. Cultures were removed to read the absorbance at 600nm. Then, plates were washed three times with water,stained with 0.1% Crystal Violet (w/v) and quantified at 550 nm after solubilization with 30% acetic acid.

Detection of PNAG production. Immunoblotting to detect PNAG production was performed as described previously (14) with some modification. Cells grown overnight on LB, then diluted to an OD of 1 and spotted in to YESCA plate and incubated for 48 hours at 26 °C. Cells were scraped from plate and normalized to an OD of 1, then pelleted and

317 resuspended in 300 µl of 0.5 M EDTA (pH 8.0). Cells were incubated for 5 min at 98 °C, and
318 centrifuged at 9000 x g for 5 min. After centrifugation, supernatants were diluted 1:3 in Tris-
319 buffered saline (TBS) and incubated with 100 µl of proteinase K (20 mg/ml) for 60 min at 65
320 °C then for 30 min at 80 °C (to inactivate the protease). The preparations were serially
321 diluted in TBS, and 5 µl were spotted on nitrocellulose membrane and let the membrane dry
322 completely. Next, membrane was blocked and incubated with an anti-PNAG antibody (kind
323 gift of Dr. Gerald B. Pier, Harvard Medical School), and an anti-human IgG (IRDye 800 CW)
324 antibody (LI-COR Biosciences, Lincoln, NE) and visualized with an Odyssey CLx imaging
325 system (LI-COR Biosciences). Following, membrane was incubated with anti-UPAB1
326 primary antibody (Ref) followed by an incubation with anti-rabbit IgG (IRDye 800 CW)
327 antibody (LI-COR Biosciences, Lincoln, NE).
328 **Scanning Electron Microscopy**. Overnight cultures on YESCA media were diluted in
329 YESCA + 4% DMSO (37) to an OD600 of 0.02 in 24 well-plate containing glass coverslips
330 and incubated at 26°C for 24 hours with shaking. Then, the media was removed, and the 24
331 well-plate was washed with 0.15 M cacodylate buffer. Cells were fixed overnight at room
332 temperature on a shaker using the fixative solution (2.5% glutaraldehyde, 2%
333 paraformaldehyde and 0.2% tannic acid in 0.15M cacodylate buffer pH 7.4 with 2mM
334 calcium chloride). Post fixation, coverslips were rinsed in 0.15 M cacodylate buffer 3 times
335 for 10 minutes each followed by a secondary fixation in 1% OsO4 in 0.15 M cacodylate
336 buffer for 45 minutes in the dark. The coverslips were then rinsed 3 times in ultrapure water
337 for 10 minutes each and dehydrated in a graded ethanol series (10%, 30%, 50%, 70%, 90%,
338 100% x2) for 10 minutes each step. Once dehydrated, the samples were loaded into a
339 critical point drier (Leica EM CPD 300, Vienna, Austria) which was set to perform 12 CO_2

exchanges at the slowest speed. Once dried, coverslips were mounted on aluminum stubs with carbon adhesive tabs and coated with 10 nm of carbon and 6 nm of iridium (Leica ACE 600, Vienna, Austria). SEM images were acquired on a FE-SEM (Zeiss Merlin, Oberkochen, Germany) at 1.5 kV and 0.1 nA.

Transmission electron microscopy and cup pili detection. Overnight cultures on YESCA media were diluted in YESCA+ 4% DMSO (37) to an OD600 of 0.02 and incubated at 26°C for 48 hours with shaking. Next cultures were washed with PBS and used for TEM and western blot. For negative staining and analysis by transmission electron microscopy, Bacterial samples were fixed with 1% glutaraldehyde (Ted Pella Inc., Redding CA) and allowed to absorb onto freshly glow discharged formvar/carbon-coated copper grids for 10 min. Grids were then washed in dH_2O and stained with 1% aqueous uranyl acetate (Ted Pella Inc.) for 1 min. Excess liquid was gently wicked off and grids were allowed to air dry. Samples were viewed on a JEOL 1200EX transmission electron microscope (JEOL USA, Peabody, MA) equipped with an AMT 8-megapixel digital camera (Advanced Microscopy Techniques, Woburn, MA). For cup pili detection, cells were resuspended in Laemmli buffer to a final OD of 10. Samples were loaded onto 15% SDS-PAGE gel for separation, transferred to a nitro-cellulose membrane and probed with polyclonal rabbit anti CupA (1:1000) and monoclonal mouse anti-RNA polymerase (1:3000, Biolegend, San 397 Diego, CA). Western blots were then probed with IRDye-conjugated anti-mouse and anti-rabbit secondary antibodies (both at 1:15,000, LI-COR Biosciences, Lincoln, NE) and visualized with an Odyssey CLx imaging system (LI-COR Biosciences).

Generation of polyclonal rabbit sera against CupA. The UPAB1 gene *cupA* was cloned into pET28a+ with a 10-histidine tag using primers SB cupA bamh1 F and SB cupA hind3

R, creating pET28-CupA10His, and electroporated into *E. coli* DH5α. pET28-CupA10His was confirmed by sequencing. E. coli Rosetta 2 cells were used for CupA purification. 1liter of LB was inoculated from an overnight culture of Rosetta 2/pET28-CupA10His at an OD_{600} of 0.05. Culture grown to an OD_{600} of ~ 0.5 before induction with 1 mM isopropyl 1-thio-β-d-galactopyranoside (IPTG). The cultures were grown for an additional 4 hours. Cells were harvested at 12000 x g for 20 min. Cells were washed with cold PBS and resuspended in binding buffer supplemented with protease inhibitor (300 mM NaCl, 10 mM imidazole, 30 mM Tris-HCl, pH 8.0). Cells were lysed with a cell disruptor using three rounds at 35 kp.s.i (Constant System Ltd., Kennesaw, GA). Cell lysates were centrifuged at 20000g (or 11000 rpm) for 20 min to collect inclusion bodies. Pellet was resuspended in binding buffer and centrifuged as described before twice. Then pellet was resuspended in binding buffer containing urea and incubated for 3 hours at 4°C with continuous stirring (6 M urea, 300 mM NaCl, 10 mM imidazole, 30 mM Tris-HCl, pH 8.0). Then, lysates were centrifuged at 35000 x g for 20 min and supernatant was filtered using 0.45 µm filter. Next, Cell lysates were passed over a nickel-NTA agarose column (Gold Bio, St. Louis, MO) equilibrated with 10 column volumes of binding buffer. The load fraction is the total cell lysate. The flow-through was collected as what passed through the column and did not bind the nickel-NTA resin. The column was washed first with 15 column volumes of washing buffer (5M urea, 20 mM imidazole, 300 mM NaCl, 30 mM Tris-HCl, pH 8.0) and second with 10 column volumes of washing buffer (4M urea, 20 mM imidazole, 300 mM NaCl, 30 mM Tris-HCl, pH 8.0). Proteins were eluted using elution buffer (2M urea, 250 mM imidazole, 300 mM NaCl, 30 mM Tris-HCl, pH 8.0). Elution fractions were analyzed by SDS-PAGE analysis and Coomassie staining. The polyacrylamide gel band corresponding to CupA-His was sent to

Antibody Research Corporation (St. Louis, MO) for peptide extraction and development of rabbit-derived polyclonal antibodies.

Growth assays. Bacteria were cultured overnight in YESCA liquid media at 26 °C under shaking conditions. Cultures were washed with PBS and diluted to an OD_{600} of 0.01 in 150 µL of YESCA liquid media in 96 well plates and incubated at 26 °C under shaking conditions. OD_{600} values were measured every 30 min for 16 hours via a BioTek microplate spectrophotometer. Three separate experiments were performed with four wells per experiment for each strain.

ACKNOWLEDGEMENTS

We acknowledge the assistance of Dr. Wandy Beatty at the Molecular Microbiology department Imaging Facility at Washington University School of Medicine in transmission electron microscopy studies, Dr. Sanja Sviben and Dr. James Fitzpatrick at the Washington University Center for Cellular Imaging (WUCCI) in scanning electron microscopy studies, which is supported by Washington University School of Medicine, The Children's Discovery Institute of University and St. Louis Children's Hospital (CDI-CORE-2015-505 and CDI-CORE-2019-813), the Foundation for Barnes-Jewish Hospital (3770). We thank Dr. Gerald B. Pier for sharing the anti-PNAG antibody.

This work was supported by grants from the National Institute of Allergy and Infectious Diseases (grants R01AI144120 and R01AI125363).

408 • **FIGURE & LEGENDS**

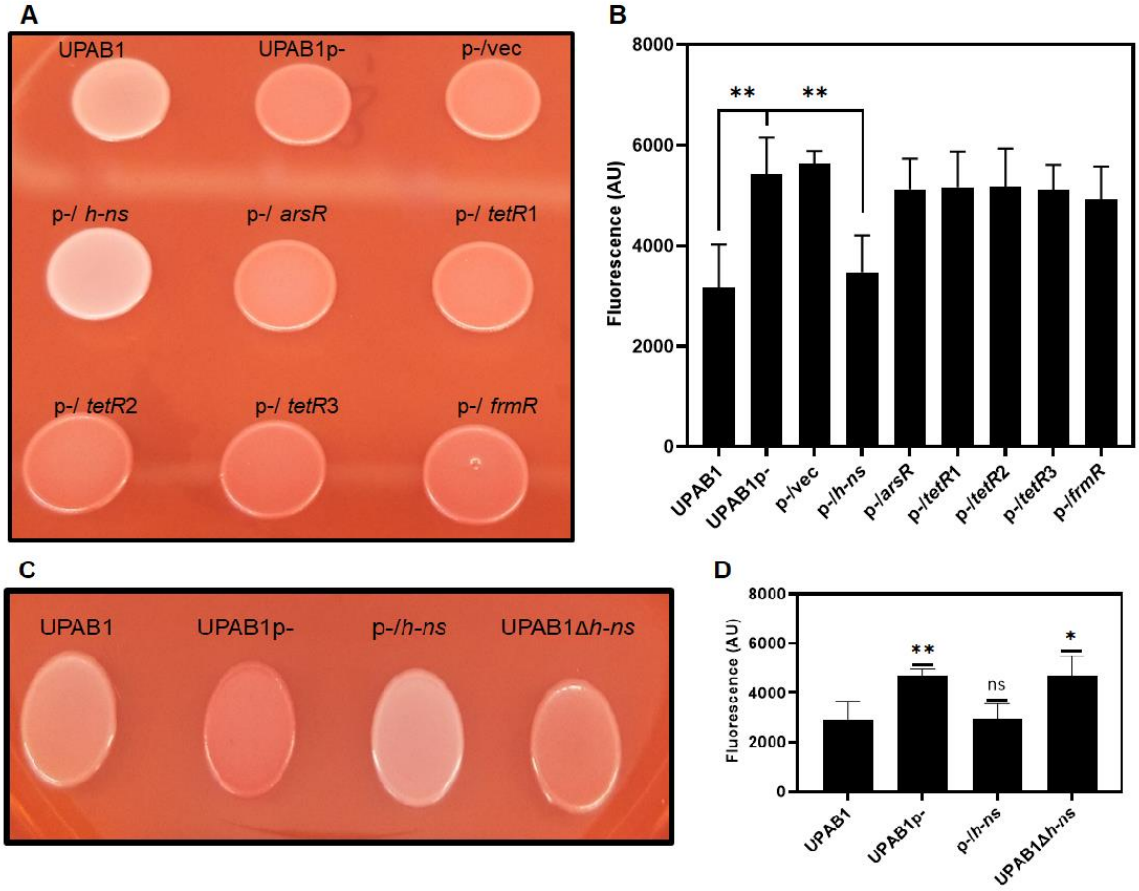

409

410 **Figure 1**. **H-NS inhibits Congo red binding.** (A & C) UPAB1 and derivatives strain
411 spotted in YESCA Congo-red agar plates. (B & D) Quantification of Congo-red binding
412 (excitation wavelength at 485 nm and the emission at 612nm). The values represent
413 the means and standard deviations from five (B) and four (D) independent
414 experiments. *t* test was performed by comparison with wild type (** p≤0.003, * p≤0.03).

415

416

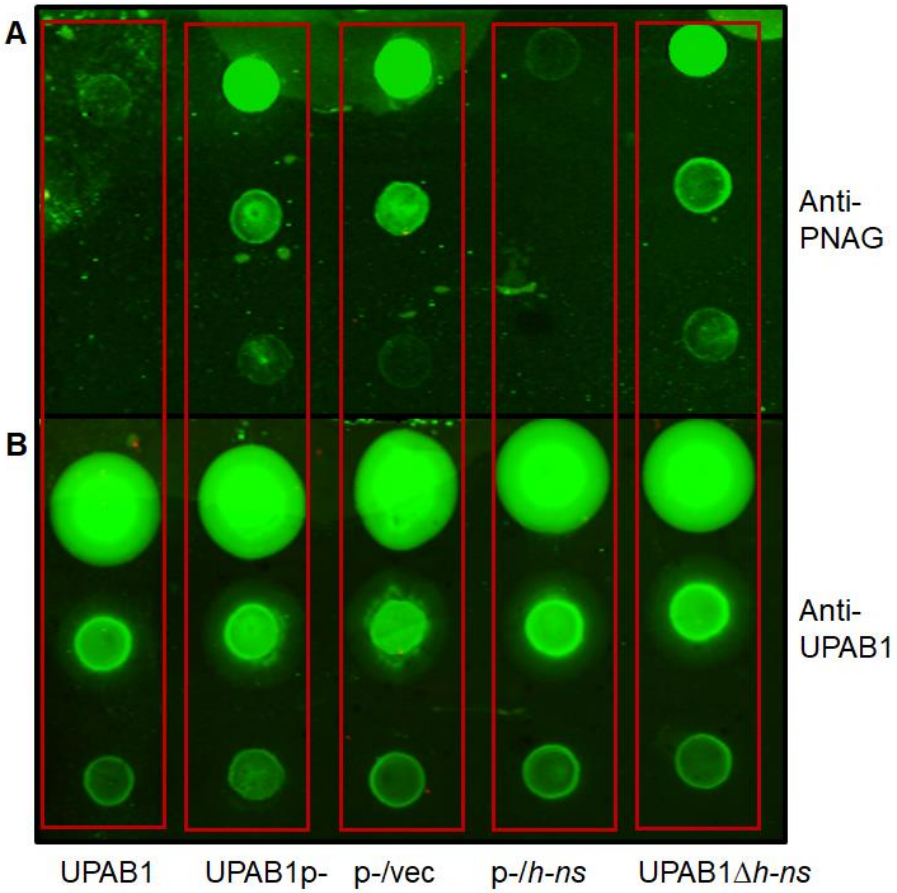

Figure 2. **H-NS reduce PNAG production**. Immunoblotting using antibodies anti-PNAG (A) and antibodies anti-UPAB1 as a loading control (B). Cells were taken from an overnight LB-agar plate at 26 °C and adjusted to an OD of 1. After treatment, 5 µl of a serial dilution were spotted on nitrocellulose membrane.

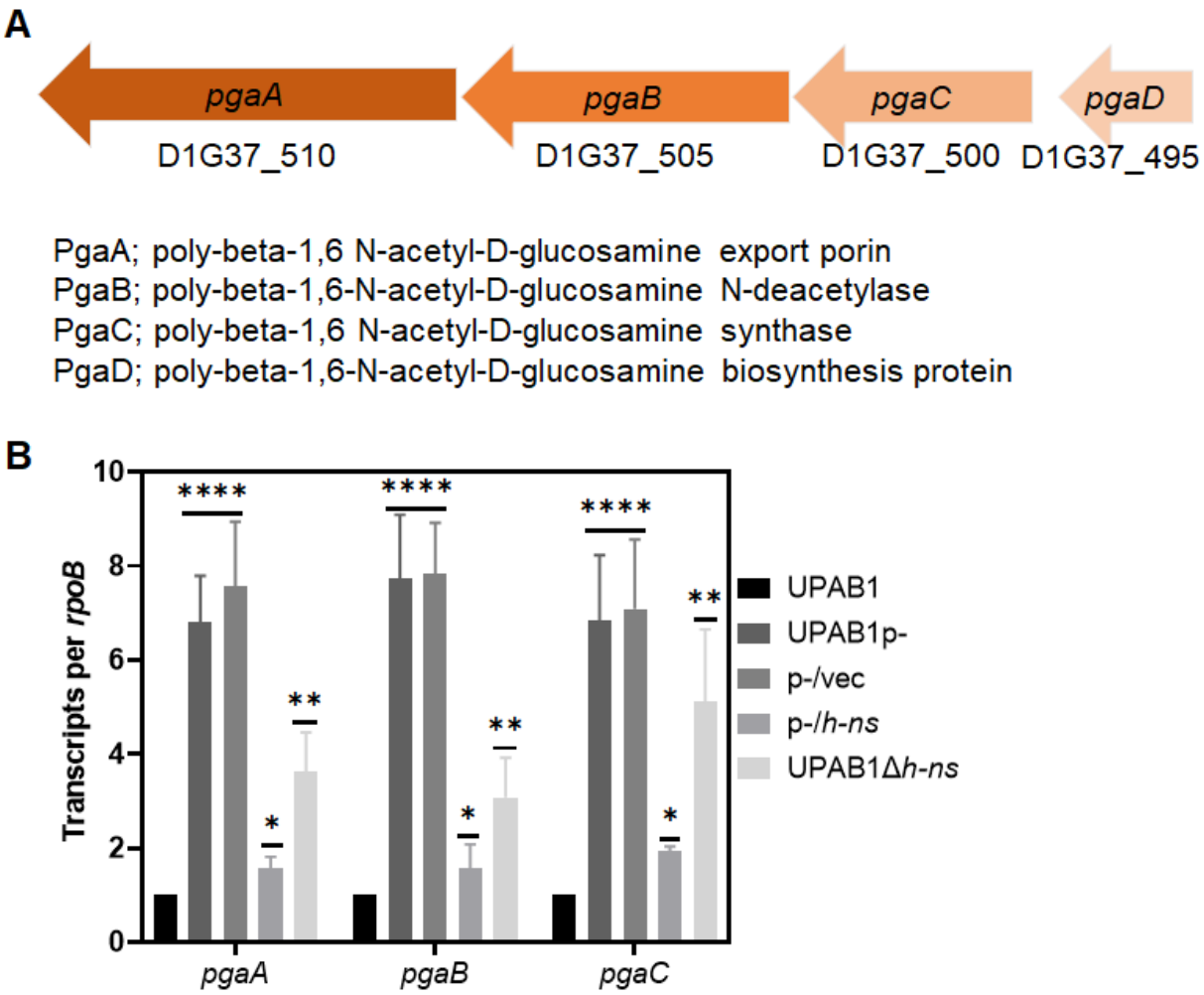

Figure 3. H-NS reduce the expression of *pnag* cluster. (A) Illustration of *pgaA-D* genes cluster. (B) *pgaABC* expression. Transcripts were measured from cells growing on LB plates at 26°C and adjusted to an OD of 1. Results are shown as rpoB-adjusted transcript values. The values represent the means and standard deviations from four independent experiments. T-test (**** p≤0.0001, ** p≤ 0.005, * p≤ 0.05).

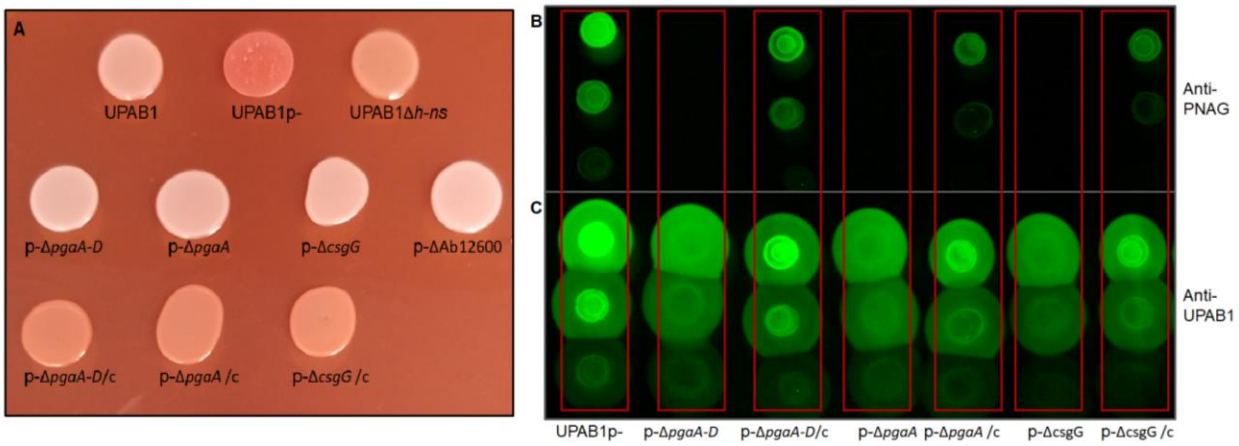

Figure 4. *pgaA-D* and curli-like clusters are involved in PNAG production. (A) phenotype on YESCA-Congo red agar plates of UPAB1p-, derivative mutant and complemented strains. PNAG production was measured using antibodies anti-PNAG (B) and antibodies anti-UPAB1 as loading control (C).

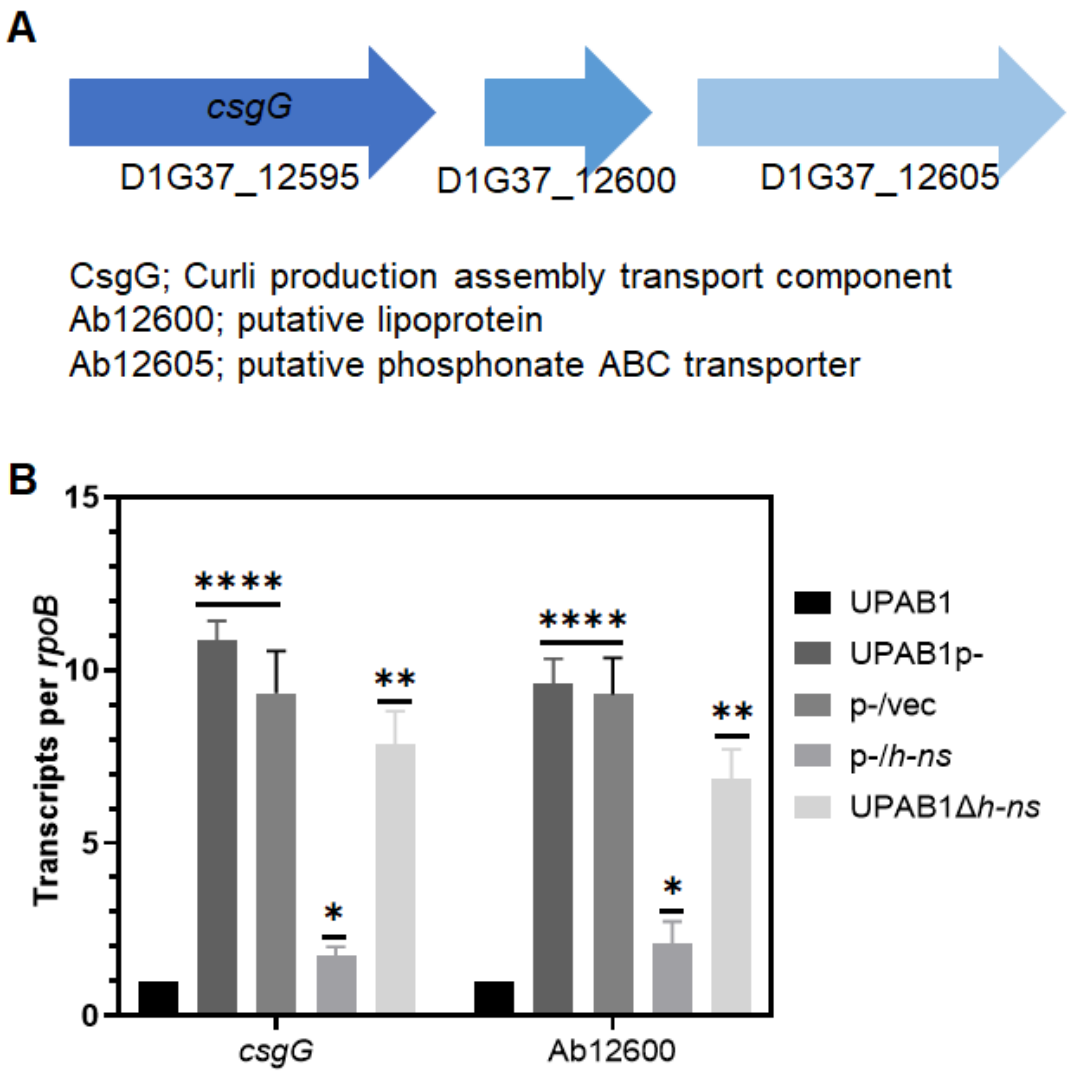

Figure 5. H-NS reduce the expression of curli-like cluster. (A) Illustration of *csgG* cluster. (B) *csgG* and Ab12600 expression. Transcripts were measured from cells growing on LB plates at 26°C and adjusted to an OD of 1. Results are shown as rpoB-adjusted transcript values. Values represent means and standard deviations from four independent experiments. T-test (**** p≤0.0001, ** p≤ 0.005, * p≤ 0.05).

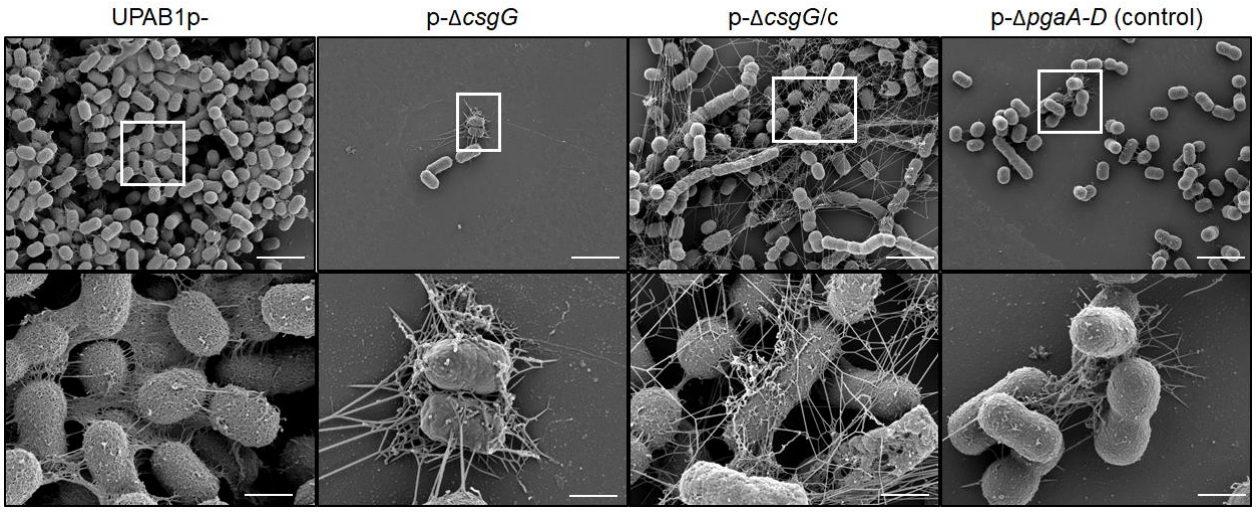

Figure 6. **CsgG and PNAG are involved in extracellular matrix production**. SEM analysis of UPAB1p-, p-ΔcsgG, p-ΔcsgG/c, and p-ΔpgaA-D (as a control). Cells grown in YESCA media with 4% DMSO in 24-well plate with glass coverslips. After overnight growth, glass coverslips were removed, washed (150 mM cacodylate buffer with 2mM CaCl2), fixed (2.5% glutaraldehyde, 2% paraformaldehyde, and 0.2% tannic acid in 150 mM cacodylate buffer (pH 7.4) with 2mM CaCl2) and treated for observation. The bottom panel is a magnification of the white square in the top panel. Scale bars are 1 μm for top panel and 200 nm for bottom panel.

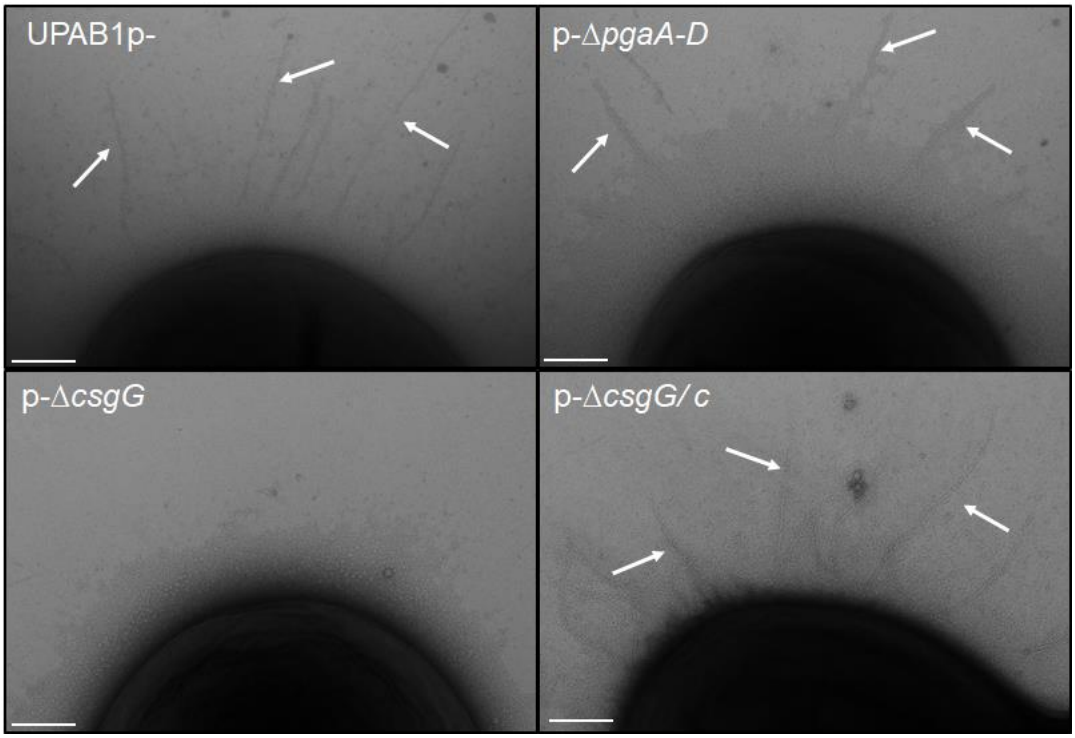

Figure 7. CsgG is involved in CUP pili formation. Transmission electron microscopic images showing CUP pili. The pili structures were absent in p-Δ*csgG* strain and restored in the complemented strain (p- Δ*csgG*/c). Cells grow for 48 hours in YESCA media supplemented with 4% DMSO with shaking at 26 °C. Sclae bar 100 nm

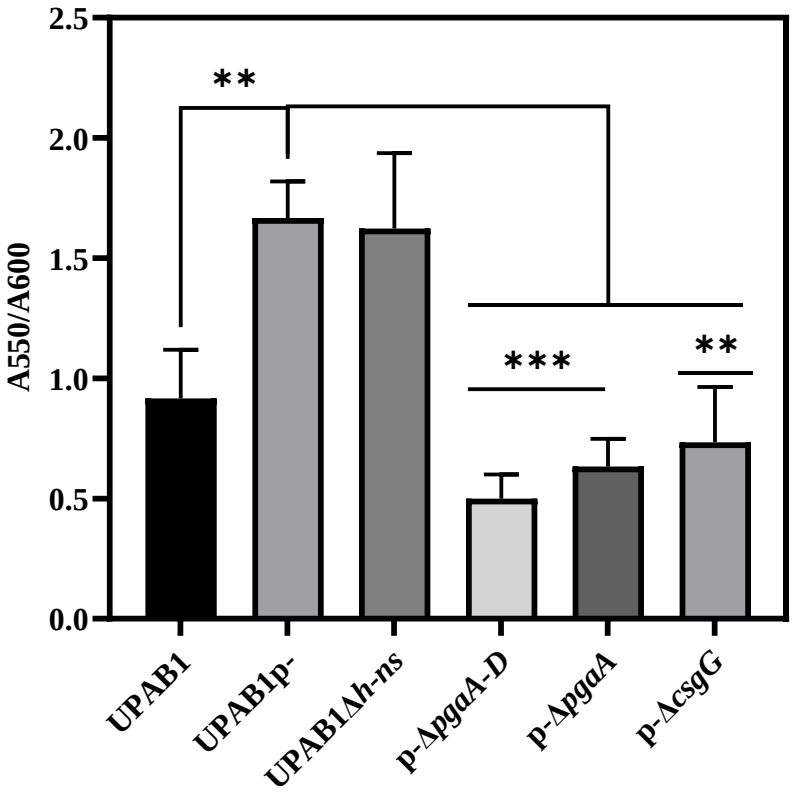

Figure 8. pAB5 reduce biofilm formation. Cells were grown for 8 hours on LB broth at 37°C in static conditions. Biofilm formation was measured by crystal violet and normalized to the growth. The values represent the mean and standard deviations from three independent experiments. T-test was performed by comparison with the pAB5- strain (*** p≤0.0005, ** p≤ 0.005)

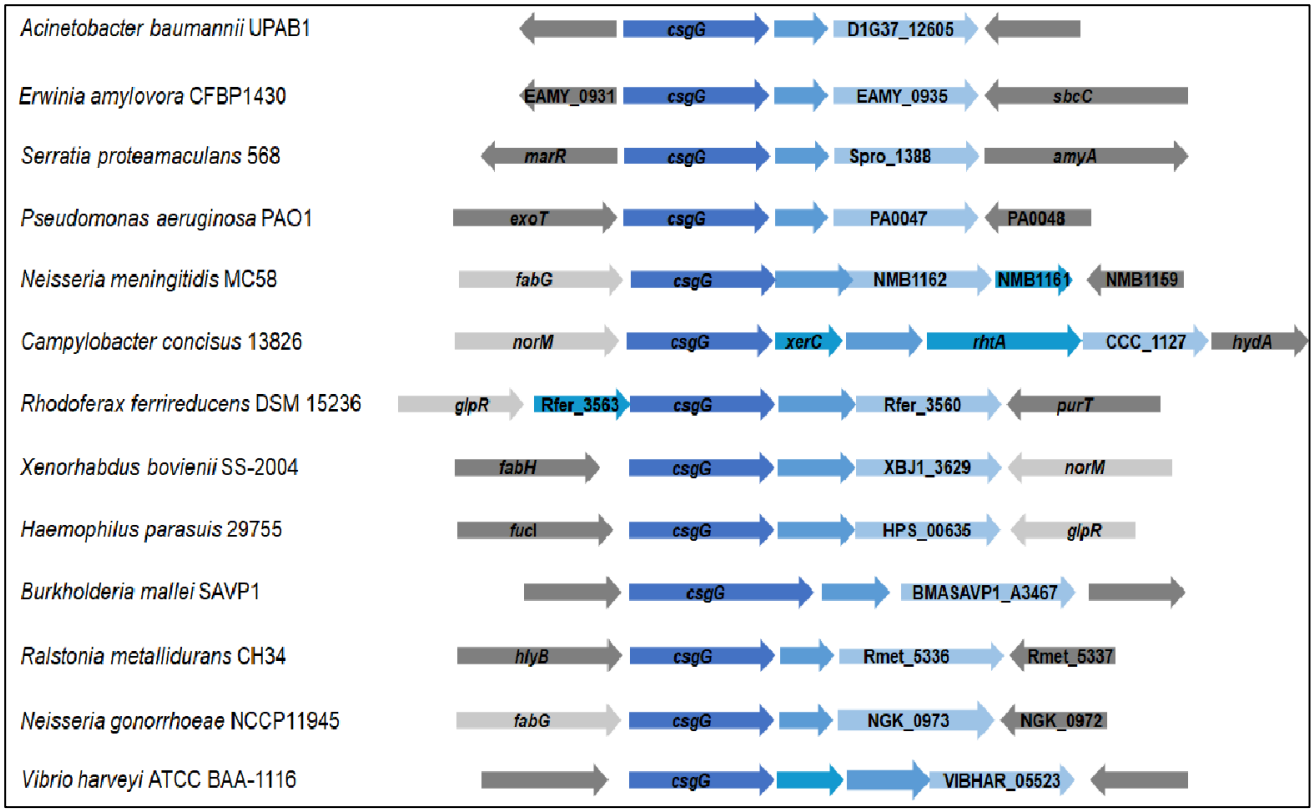

Figure 9. **Distribution of *csgG* cluster in Gram- negative bacteria**. The *csgG* cluster is indicated in blue.

538 • **REFERENCES**

539 1. Giammanco A, Calà C, Fasciana T, Dowzicky MJ. 2017. Global Assessment of the
540 Activity of Tigecycline against Multidrug-Resistant Gram-Negative Pathogens between
541 2004 and 2014 as Part of the Tigecycline Evaluation and Surveillance Trial. mSphere
542 2.
543 2. Rolain JM, Diene SM, Kempf M, Gimenez G, Robert C, Raoult D. 2013. Real-time
544 sequencing to decipher the molecular mechanism of resistance of a clinical pan-drug-
545 resistant Acinetobacter baumannii isolate from Marseille, France. Antimicrobial Agents
546 and Chemotherapy 57:592–596.
547 3. Blackwell GA, Hamidian M, Hall RM. 2016. IncM Plasmid R1215 Is the Source of
548 Chromosomally Located Regions Containing Multiple Antibiotic Resistance Genes in
549 the Globally Disseminated Acinetobacter baumannii GC1 and GC2 Clones. mSphere
550 1.
551 4. Wright MS, Iovleva A, Jacobs MR, Bonomo RA, Adams MD. 2016. Genome
552 dynamics of multidrug-resistant Acinetobacter baumannii during infection and
553 treatment. Genome Medicine 8.
554 5. Norman A, Hansen LH, Sørensen SJ. 2009. Conjugative plasmids: Vessels of the
555 communal gene pool. Philosophical Transactions of the Royal Society B: Biological
556 Sciences. Royal Society.
557 6. Luque A, Paytubi S, Sánchez-Montejo J, Gibert M, Balsalobre C, Madrid C. 2019.
558 Crosstalk between bacterial conjugation and motility is mediated by plasmid-borne
559 regulators. Environmental Microbiology Reports 11:708–717.
560 7. Smalla K, Jechalke S, Top EM. 2015. Plasmid Detection, Characterization, and
561 Ecology. Microbiology Spectrum 3.
562 8. Orlek A, Stoesser N, Anjum MF, Doumith M, Ellington MJ, Peto T, Crook D,
563 Woodford N, Sarah Walker A, Phan H, Sheppard AE. 2017. Plasmid classification in an
564 era of whole-genome sequencing: Application in studies of antibiotic resistance
565 epidemiology. Frontiers in Microbiology. Frontiers Research Foundation.
566 9. Weber BS, Ly PM, Irwin JN, Pukatzki S, Feldman MF. 2015. A multidrug resistance
567 plasmid contains the molecular switch for type VI secretion in Acinetobacter baumannii.
568 Proceedings of the National Academy of Sciences of the United States of America
569 112:9442–9447.
570 10. di Venanzio G, Moon KH, Weber BS, Lopez J, Ly PM, Potter RF, Dantas G,
571 Feldman MF. 2019. Multidrug-resistant plasmids repress chromosomally encoded
572 T6SS to enable their dissemination. Proceedings of the National Academy of Sciences
573 of the United States of America 116:1378–1383.
574 11. di Venanzio G, Flores-Mireles AL, Calix JJ, Haurat MF, Scott NE, Palmer LD,
575 Potter RF, Hibbing ME, Friedman L, Wang B, Dantas G, Skaar EP, Hultgren SJ,
576 Feldman MF. 2019. Urinary tract colonization is enhanced by a plasmid that regulates

577 uropathogenic Acinetobacter baumannii chromosomal genes. Nature Communications
578 10.
579 12. Doyle M, Fookes M, Ivens A, Mangan MW, Wain J, Dorman CJ. 2007. An H-NS-
580 like Stealth Protein Aids Horizontal DNA Transmission in Bacteria. Science 315:251.
581 13. Lucidi M, Runci F, Rampioni G, Frangipani E, Leoni L, Visca P. 2018. New shuttle
582 vectors for gene cloning and expression in multidrug-resistant Acinetobacter species.
583 Antimicrobial Agents and Chemotherapy 62.
584 14. Choi AHK, Slamti L, Avci FY, Pier GB, Maira-Litrán T. 2009. The pgaABCD locus of
585 Acinetobacter baumannii encodes the production of poly-β-1-6-N-acetylglucosamine,
586 which is critical for biofilm formation. Journal of Bacteriology 191:5953–5963.
587 15. Whitney JC, Howell PL. 2013. Synthase-dependent exopolysaccharide secretion in
588 Gram-negative bacteria. Trends in Microbiology.
589 16. Barnhart MM, Chapman MR. 2006. Curli biogenesis and function. Annual Review
590 of Microbiology.
591 17. Evans ML, Chapman MR. 2014. Curli biogenesis: Order out of disorder. Biochimica
592 et Biophysica Acta - Molecular Cell Research 1843:1551–1558.
593 18. van Gerven N, Klein RD, Hultgren SJ, Remaut H. 2015. Bacterial amyloid
594 formation: Structural insights into curli biogensis. Trends in Microbiology. Elsevier Ltd.
595 19. Vella P, Rudraraju RS, Lundbäck T, Axelsson H, Almqvist H, Vallin M, Schneider
596 G, Schnell R. 2021. A FabG inhibitor targeting an allosteric binding site inhibits several
597 orthologs from Gram-negative ESKAPE pathogens. Bioorganic and Medicinal
598 Chemistry 30.
599 20. Ge B, McDermott PF, White DG, Meng J. 2005. Role of efflux pumps and
600 topoisomerase mutations in fluoroquinolone resistance in Campylobacter jejuni and
601 Campylobacter coli. Antimicrobial Agents and Chemotherapy 49:3347–3354.
602 21. Cai X, Lu J, Wu Z, Yang C, Xu H, Lin Z, Shen Y. 2013. Structure of Neisseria
603 meningitidis lipoprotein GNA1162. Acta Crystallographica Section F: Structural Biology
604 and Crystallization Communications 69:362–368.
605 22. Vial L, Hommais F. 2020. Plasmid-chromosome cross-talks. Environmental
606 Microbiology. Blackwell Publishing Ltd.
607 23. Ro¨mling U, Ro¨mling R, Bian Z, Hammar M, Sierralta WD, Normark S. 1998. Curli
608 Fibers Are Highly Conserved between Salmonella typhimurium and Escherichia coli
609 with Respect to Operon Structure and RegulationJOURNAL OF BACTERIOLOGY.
610 24. Sigma S-dependent growth-phase induction of the csgBA promoter in Escherichia
611 coli can be achieved in vivo by sigma 70 in the absence of the nucleoid-associated
612 protein H-NS.
613 25. Gerstel U, Park C, Römling U. 2003. Complex regulation of csgD promoter activity
614 by global regulatory proteins. Molecular Microbiology 49:639–654.

26. Olsen A, Arnqvist A, Hammar M, Sukupotvi^ S, Normark' S. 1993. The RpoS Sigma factor relieves H-NS-mediated transcriptional repression of csgA, the subunit gene of fibronectin-binding curii in Escherichia coliMolecular Microbiology.
27. Desai SK, Winardhi RS, Periasamy S, Dykas MM, Jie Y, Kenney LJ. 2016. The horizontally-acquired response regulator SsrB drives a Salmonella lifestyle switch by relieving biofilm silencing https://doi.org/10.7554/eLife.10747.001.
28. Desai SK, Kenney LJ. 2019. Switching Lifestyles Is an in vivo Adaptive Strategy of Bacterial Pathogens. Frontiers in Cellular and Infection Microbiology. Frontiers Media S.A.
29. Hardy GG, Allen RC, Toh E, Long M, Brown PJB, Cole-Tobian JL, Brun Y v. 2010. A localized multimeric anchor attaches the Caulobacter holdfast to the cell pole. Molecular Microbiology 76:409–427.
30. Hardy GG, Toh E, Berne C, Brun Y v. 2018. Mutations in sugar-nucleotide synthesis genes restore holdfast polysaccharide anchoring to Caulobacter crescentus holdfast anchor mutants. Journal of Bacteriology 200.
31. Sulkowski NI, Hardy GG, Brun Y v, Bharat TAM. 2019. A Multiprotein Complex Anchors Adhesive Holdfast at the Outer Membrane of Caulobacter crescentus. jb.asm.org 1 Journal of Bacteriology 201:112–131.
32. Tucker AT, Nowicki EM, Boll JM, Knauf GA, Burdis NC, Stephen Trent M, Davies BW. 2014. Defining gene-phenotype relationships in acinetobacter baumannii through one-step chromosomal gene inactivation. mBio 5:1–9.
33. Kumar A, Dalton C, Cortez-Cordova J, Schweizer HP. 2010. Mini-Tn7 vectors as genetic tools for single copy gene cloning in Acinetobacter baumannii. Journal of Microbiological Methods 82:296–300.
34. Ducas-Mowchun K, Malaka P, Silva D, Crisostomo L, Fernando DM, Chao T-C, Pelka P, Schweizer HP, Kumar A. 2019. Next Generation of Tn7-Based Single-Copy Insertion Elements for Use in Multi- and Pan-Drug-Resistant Strains of Acinetobacter baumannii.
35. Nenninger AA, Robinson LS, Hultgren SJ. 2008. Localized and efficient curli nucleation requires the chaperone-like amyloid assembly protein CsgF.
36. Zhou Y, Blanco LP, Smith DR, Chapman MR. 2012. Bacterial amyloids. Methods in Molecular Biology 849:303–320.
37. Lim JY, May JM, Cegelski L. 2012. Dimethyl sulfoxide and ethanol elicit increased amyloid biogenesis and amyloid-integrated biofilm formation in Escherichia coli. Applied and Environmental Microbiology 78:3369–3378.

- **SUPPLEMENTAL MATERIAL**

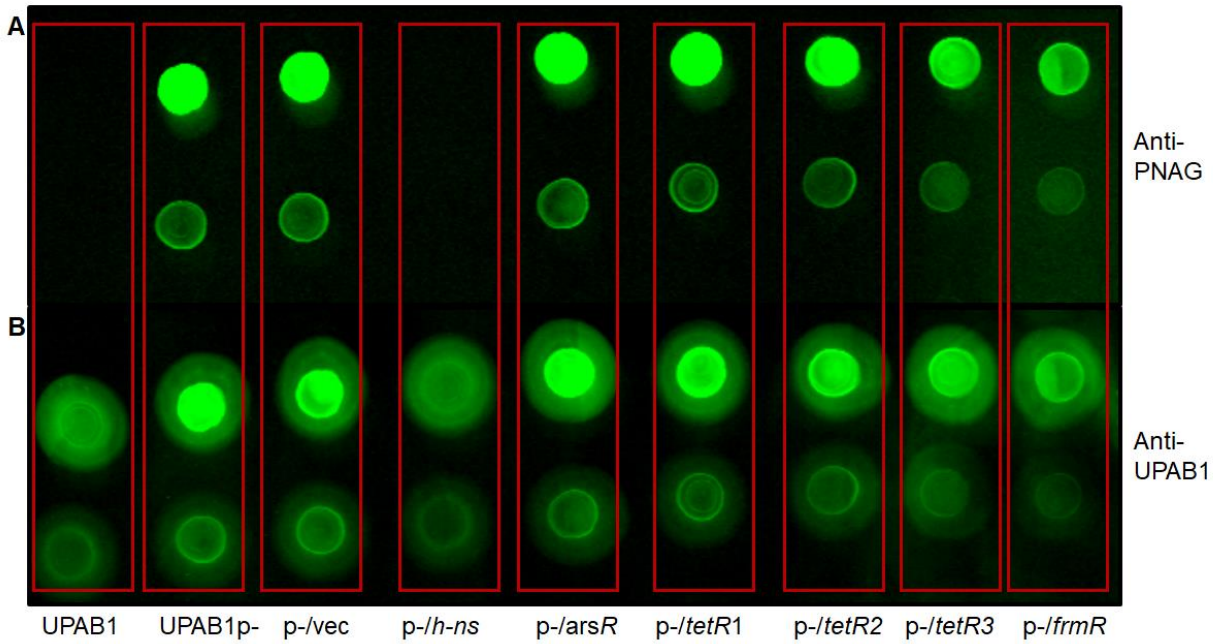

Figure S1. H-NS reduce PNAG production. UPAB1, UPAB1p-, and UPAB1p- empty vector (p-/vec) or the vector expressing the pAB5 regulators. Immunoblots using antibodies anti-PNAG (A) and antibodies anti-UPAB1 as loading control (B). Cells were taken from overnight LB-agar plates incubated at 26 °C and adjusted to OD 1.

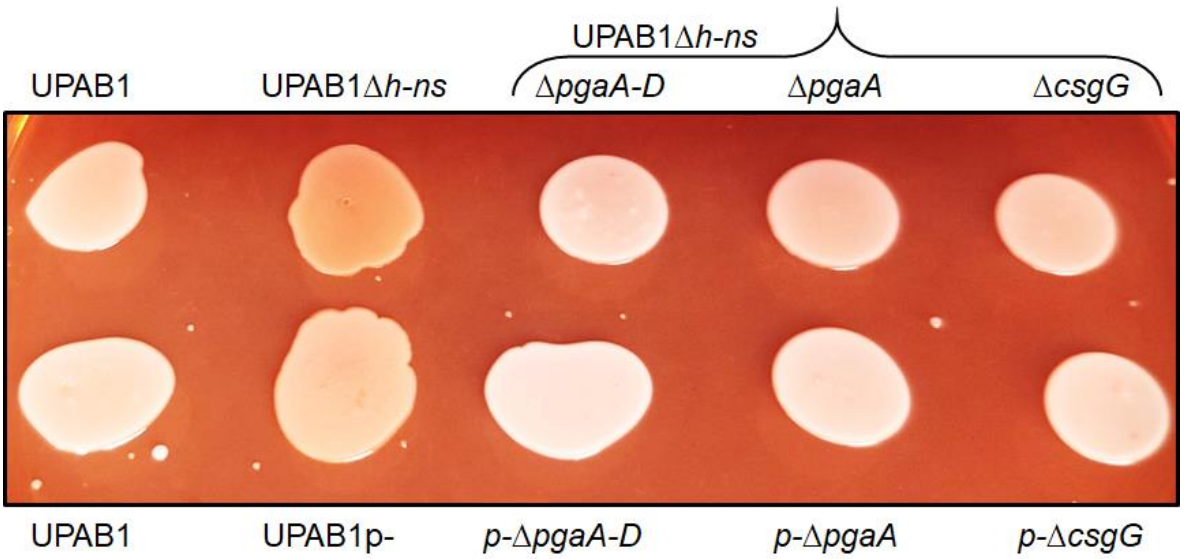

Figure S2. PgaA-D and CsgG like clusters are involved in Congo-red binding. Deletions of pgaA-D, pgaA and csgG were made in UPAB1Δ*h-ns* background (top panel) and UPAB1p- background. Cells were incubated for 48 hours at 26°C on YESCA-Congo-red agar plates.

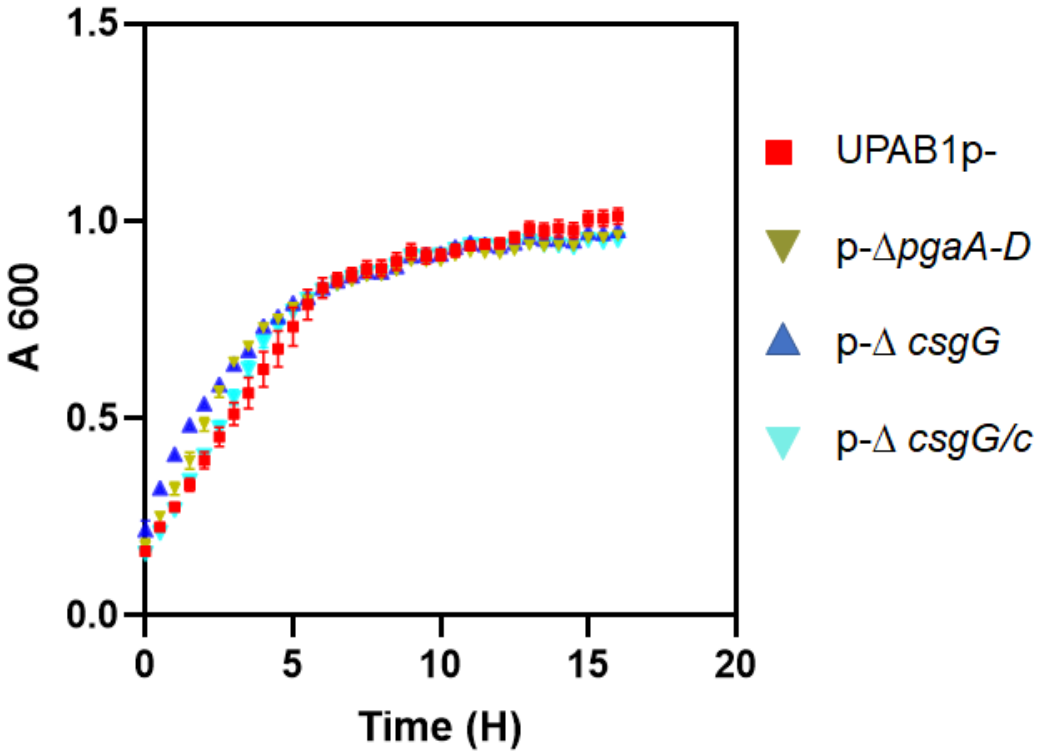

680

681 **FigureS3**. Growth curves of UPAB1p- and derivative mutant strains in YESCA-DMSO
682 media, measured by OD600. The graphs represent the mean and standard deviation of
683 three replicates.

684

685

686

687

688

689

690

691

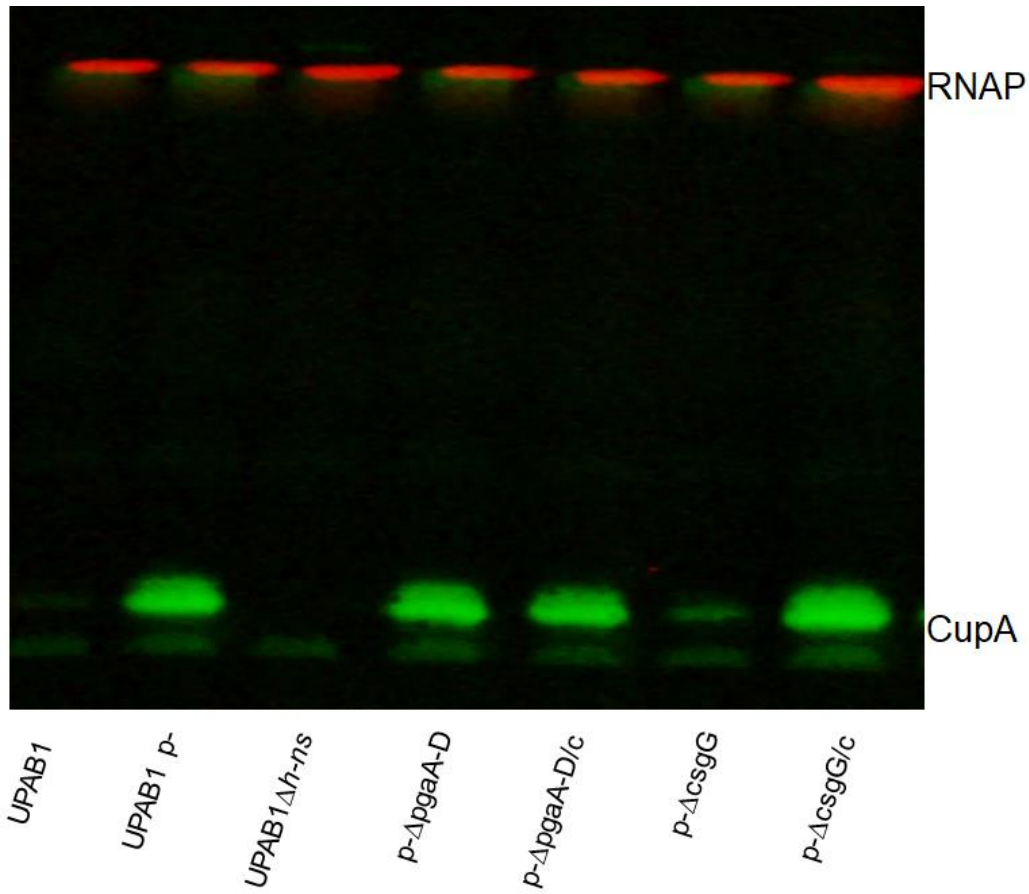

692

693 **Figure S4**. pAB5 inhibits CUP pili formation. Western blot of OD-normalized whole cell.
694 Western blot probing for CupA (the Usher protein from Cup 2 pili). RNAP is included as
695 loading control.

696

697

698

699

700

701

702

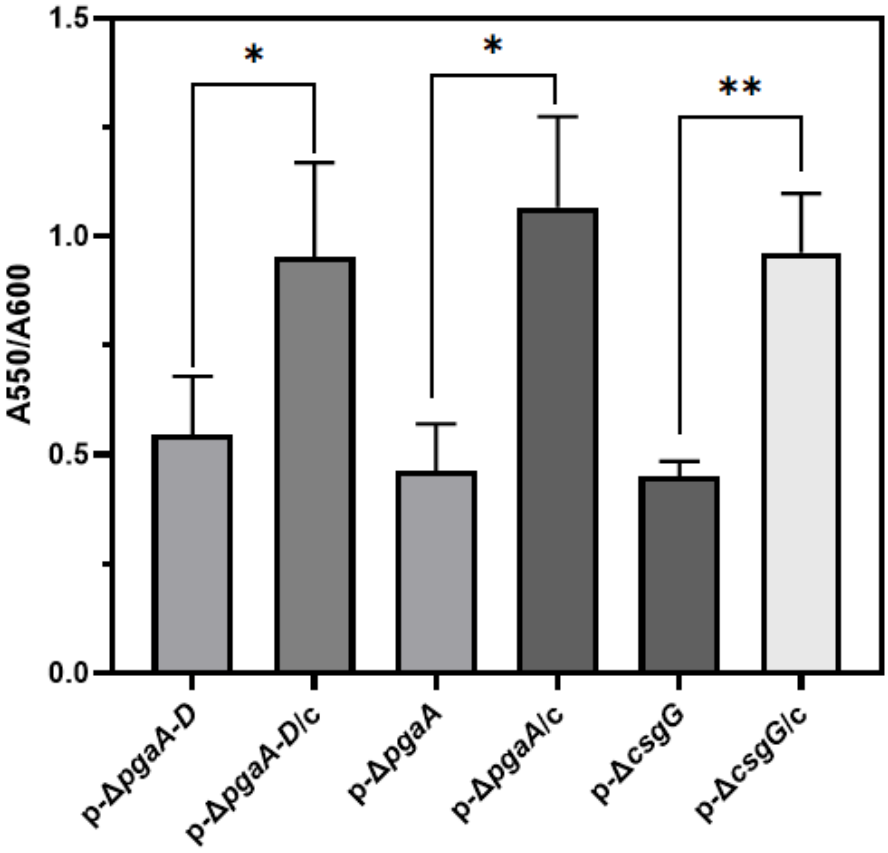

Figure S5. Biofilm formation in UPAB1p- mutants and complemented strains. Cells were grown for 8 hours on LB broth at 37°C under static conditions. Biofilm formation was measured by the crystal violet binding and normalized to the OD600. The values represent the mean and standard deviations from three independent experiments. Statistical analysis by t test was performed by comparison with the pAB5- strain (** p≤0.005, * p≤ 0.05).

Table S1. List of regulators identified in pAB5

Accession number	Description	Protein name
D1G37_RS18580	H-NS histone family protein	H-NS
D1G37_RS18620	TetR/AcrR family transcriptional regulator	TetR1
D1G37_RS18650	TetR/AcrR family transcriptional regulator	TetR2
D1G37_RS18810	TetR family transcriptional regulator	TetR3
D1G37_RS18815	ArsR family transcriptional regulator	ArsR
D1G37_RS18965	metal/formaldehyde-sensitive family transcriptional regulator	FrmR

Table S2. Bacterial strains used in this study.

Strain	Relevant properties	Reference
UPAB1	MDR Urine isolate with pAB5 plasmid	(1)
UPAB1p- (p-)	UPAB1derivative strain without pAB5	(1)
UPAB1Δ*h-ns*	UPAB1 containing an unmarked *h-ns* deletion	this study
p-/vec	UPAB1p- containing the pVRL2 expression vector	this study
p-/*h-ns*	p- expressing *h-ns* in pVRL2	this study
p-/*tetR*1	p- expressing *tetR*1 in pVRL2	this study
p-/*tetR*2	p- expressing *tetR*2 in pVRL2	this study
p-/*tetR*3	p- expressing *tetR*3 in pVRL2	this study
p-/*ars*R	p- expressing *arsR* in pVRL2	this study
p-/*frm*R	p- expressing *frm*R in pVRL2	this study
p-Δ*pgaA-D*	p- containing an unmarked *pgaA-D* deletion	this study
p-Δ*pgaA*	p- containing an unmarked *pgaA* deletion	this study
p-Δ*csgG*	p- containing an unmarked *csgG* deletion	this study
p-ΔAb*12600*	p- containing an unmarked D1G37_12600 deletion	this study
p+Δ*h-ns* Δ*pgaA-D*	UPAB1 containing an unmarked *h-ns* and *pgaA-D* deletion	this study
p+Δ*h-ns* Δ*pgaA*	UPAB1 containing an unmarked *h-ns* and *pgaA* deletion	this study
p+Δ*h-ns* Δ*csgG*	UPAB1 containing an unmarked *h-ns* and *csgG* deletion	this study
p-Δ*pgaA-D*/c	p-Δ*pgaA-D* complemented	this study
p-Δ*pgaA*/c	p-Δ*pgaA* complemented	this study
p-Δ*csgG*/c	p-ΔcsgG complemented	this study

Table S3. Bacterial plasmids used in this study.

Plasmid	Relevant properties	Reference
pVRL2	Expression vector in *Acinetobacter*; Gm^r	(2)
pVRL2/*h-ns*	pVRL2 containing *h-ns*	this study
pVRL2/*tetR*1	pVRL2 containing *terR1*	
pVRL2/*tetR*2	pVRL2 containing *tetR*2	
pVRL2/*tetR*3	pVRL2 containing *tetR*3	
pVRL2/*arsR*	pVRL2 containing *arsR*	
pVRL2/*frmR*	pVRL2 containing *frmR*	
pAT03	pMMB67EH with FLP recombinase Hyg^r	(ref)
pAT04	pMMB67EH with RecAb system, Hyg^r	(ref)
pUC18T-miniTn7T-Gm	mobilizable mini-Tn7 vector, Gm^r	(ref)
pUC18T-miniTn7-*pgaA-D*		this study
pUC18T-miniTn7- *pgaA*		this study
pUC18T-miniTn7-*csgG*		this study
pTNS2	Tn7 transposase- expressing helper plasmid, Amp^r	(ref)
pRK2013	RK2 derivative, Km^r; self-transmissible	(ref)
pET28 a+		Novagen
pET28 a-CupA		this study